

Co-published by Institute of Fluid-Flow Machinery Polish Academy of Sciences

Committee on Thermodynamics and Combustion

Polish Academy of Sciences

Copyright@2025 by the Authors under licence CC BY-NC-ND 4.0

http://www.imp.gda.pl/archives-of-thermodynamics/



Forecasting the energy efficiency of an earth-air heat exchanger with integrated twisted tabs using machine learning techniques

Fatima Benali Kouchih, Khadidja Boualem*, Malika Seddik Bouchouicha, Yasmine Bentouba, Abdhalim Soussa, Abbes Azzi

Aero Hydrodynamic Naval Laboratory (LAHN), University of Science and Technology of Oran Mohamed Boudiaf (USTO-MB), Faculty of Mechanical Engineering, BP1505 El-Mnaouar, Oran 31000, Algeria

*Corresponding author email: khadoc07@yahoo.fr

Received: 08.03.2025; revised: 06.08.2025; accepted: 07.08.2025

Abstract

This study investigates the potential of machine learning models as efficient alternatives to traditional computational methods for evaluating the performance of earth-air heat exchanger systems. A validated numerical model was used to simulate system behaviour under varying parameters, including soil type, pipe material, number of internal twisted tabs and outlet temperature. Based on these simulations, a dataset comprising 216 entries was generated to train three machine learning models: support vector regression, gradient boosting and decision trees. The gradient boosting model achieved the highest predictive accuracy, with a root mean square error of 0.0188 and a mean absolute error of 0.0138. Support vector regression and decision trees also demonstrated strong performance, with prediction accuracies of 97% and 96%, respectively. Additionally, the proposed earth-air heat exchanger design with twisted tabs showed superior thermal performance compared to the conventional configuration. Over extended operation, the temperature difference between inlet and outlet exceeded 7°C, with the new configuration system incorporating 10 tabs yielding optimal performance. This configuration led to more than a 10% improvement in thermal efficiency and an increase of approximately 25% in the heat transfer coefficient. These results confirm that integrating machine learning with advanced earth-air heat exchanger designs offers a reliable and computationally efficient approach for enhancing system performance.

Keywords: Machine learning; Earth-air heat exchanger; Twisted tabs; Heat transfer; Dataset

Vol. 46(2025), No. 3, 127-139; doi: 10.24425/ather.2025.156584

Cite this manuscript as: Benali Kouchih, F., Boualem, K., Seddik Bouchouicha, M., Bentouba, Y., Soussa, A., & Azzi, A. (2025). Forecasting the energy efficiency of an earth-air heat exchanger with integrated twisted tabs using machine learning techniques. *Archives of Thermodynamics*, 46(3), 127–139.

1. Introduction

Heat transfer has always played a crucial role in industry and mechanical systems. It enables the transfer of thermal energy between substances without direct contact or mixing [1]. Applications of heat exchangers span various sectors, including the chemical industry, food processing, space heating, heat recovery systems, vegetable drying, paper treatment and air conditioning

[2]. The design of heat exchangers can vary significantly depending on their type and intended function. As a result, numerous configurations have been developed by modifying shapes, sizes, materials, and incorporating various types of flow disruptors or mixers into the heat exchange regions.

Methods for enhancing the thermal performance of heat exchangers are generally classified into three categories: active, passive and combined enhancement techniques. Active methods

Nomenclature

c_p – pipe thermal specific heat, kJ/(kg K)

 $C_{\varepsilon l}$, $C_{\varepsilon 2}$, C_{μ} – constants of the k– ε model

D – pipe diameter, m

h – heat transfer coefficient, W/(m²·K)

k – turbulent kinetic energy, (J/kg)

L – length of the pipe, m

Pr - Prandtl number

Qc -cooling capacity, W

T – temperature, K

 u_i - velocity component in the *i*-th direction, m/s

V − flow velocity of the fluid, m/s

Z – pipe buried depth, m

Greek symbols

ρ – density of the fluid, kg/m³

λ – thermal conductivity, W/(m K)

 ε – dissipation rate of k, W/kg

 μ – viscosity, kg/(m s)

 σ_k , σ_{ε} – turbulent Prandtl numbers for k– ε

Subscripts and Superscripts

in - inlet

out - outlet

s − soil

p – pipe

t - turbulent

Abbreviations and Acronyms

AL - aluminium

ANN- artificial neural networks

CFD - computational fluid dynamics

EAHE- earth-to-air heat exchanger

EAHET- earth air heat exchanger with twisted tab

HDPE- high-density polyethylene

MAE - mean absolute error

NN – neural network

NSE – Nash-Sutcliffe efficiency

PVC - polyvinyl chloride

RANS - Reynolds-averaged Navier-Stokes equations

RMSE - root mean square error

RSM - response surface methodology

SD - standardised value

SVR - support vector regression

rely on external power sources and employ techniques such as magnetic fields, auxiliary mechanical systems, fluid injection or surface vibrations. In contrast, passive methods are more commonly studied and applied, as they require no additional energy input and are relatively easy to implement [3,4]. Aziz and Rehman [5] numerically simulated a small heat exchanger equipped with six baffles. By sequentially removing each baffle plate, they found that removing the inlet and outlet baffles had minimal impact on pressure drop, while removing the central baffles caused significant pressure fluctuations. Muszyński and Dorao [6] conducted an experimental study to evaluate the performance of a heat exchanger module with an enhanced surface. Their results indicated a 60% improvement in heat flux. The enhancement of heat transfer in various innovative heat exchanger designs using computational fluid dynamics (CFD) has also been widely documented in the literature. A comparative study conducted by Serrao et al. [7] using ANSYS Fluent evaluated the performance of smooth and corrugated tubes. Their CFD analysis showed that the corrugated tube exhibited a 54.7% increase in the overall heat transfer coefficient compared to the smooth tube. Vignesh et al. [8] and Wang et al. [9] used computational methods to investigate the impact of dimples on the thermal performance of heat exchangers. They found that dimpled tubes led to a higher temperature rise and pressure drop compared to smooth tubes. Kumar et al. [10] analysed the heat transfer and flow characteristics of double helically coiled tube heat exchangers. Extensive research has also been conducted on the performance and efficiency of tubes operating in turbulent flow regimes [11]. Kishan et al. [12] performed a numerical study on different flow patterns inside the tubes of shell-and-tube heat exchangers. Sharma et al. [13] examined flow patterns, pressure drops, and heat transfer coefficients in both staggered and inline configurations of shell-and-tube heat exchangers. Larwa and Kupiec [14] proposed analytical relationships based on Green's

function theory to model heat transfer in spiral ground heat exchangers. Rahimi et al. [15] carried out both numerical and experimental investigations on four types of inserts: classic, perforated, notched and jagged twisted tapes, and found that the jagged insert yielded the best heat transfer performance. Molcrette and Autier [16] introduced a new formula to estimate earth energy for earth—air pipe heat exchangers during winter heating. Their study emphasised how various parameters affect the proper sizing of the system. In an experimental study, Nawaz and Prakach [17] tested three horizontal PVC pipes of different diameters to evaluate the thermal performance of an earth-to-air heat exchanger, concluding that the smallest pipe diameter provided the highest efficiency.

In recent years, artificial intelligence (AI) has attracted considerable attention due to its exceptional ability to deliver positive outcomes across various fields. Among AI techniques, machine learning (ML) has been widely adopted by researchers for identifying optimal process parameters [18]. This approach offers significant advantages, including reduced computational time, enhanced productivity and minimal human intervention. Of the many ML techniques available, supervised and unsupervised learning models are the most commonly employed in thermal system research [19,20]. In the context of heat exchangers, the heating or cooling capacity, typically quantified by the heat transfer rate, is a critical performance parameter.

Numerous studies have applied machine learning methods to predict heat exchanger performance. For instance, Karami et al. [21] assessed the effectiveness of an artificial neural network (ANN) in predicting heat transfer. Their experimental and numerical investigations on tubes with butterfly inserts considered the influence of insert inclination angle and Reynolds number variation. The ANN, developed in MATLAB, achieved a training error of 0.109% and a testing error of 0.509%, indicating high agreement between predicted and experimental results.

Li et al. [22] and Shojaeefard et al. [23] focused on predicting cooling capacity. Li et al. implemented a neural network based on response surface methodology (RSM), while Shojaeefard et al. explored different ANN architectures.

Deb et al. [24] employed a regression-based classification ML model to predict output parameters from a given set of inputs. The model's accuracy was evaluated using the residual sum of squares method, with results showing strong agreement between predicted and simulated values for fluid outlet temperature and pressure drop. Liao et al. [25] combined multilayer perceptron (MLP) networks with Bayesian optimisation to design an optimal near-field thermal radiative modulator, considering variables such as rotation angle, layer thickness, and gap distance between layers.

Ren et al. [26] explored advanced techniques by integrating reinforcement learning with proximal policy optimisation (PPO) and the non-Oberbeck–Boussinesq (NOB) approximation. They achieved a 76% improvement in heat transfer by developing a smart active flow control system for laminar flow enhancement. Wang and Vafai [27] applied support vector regression (SVR) algorithms in conjunction with thermal simulations to accurately predict temperature variations in hotspots within multilayer 3D electronic chips.

Çolak et al. [28] employed the Levenberg-Marquardt training algorithm to develop two predictive models aimed at estimating key performance parameters, including the overall heat transfer coefficient, pressure drops on both the tube and annulus sides, and the total cost. Each model was trained using a dataset comprising 438 samples and incorporated a hidden layer with 15 neurons. Model 1 achieved estimation deviations of 0.16% for the overall heat transfer coefficient, -0.23% for the tube-side pressure drop, -0.02% for the annulus-side pressure drop, and -0.003% for the overall cost. Model 2 yielded deviations of 0.02%, -0.18%, -0.16%, and -0.15%, respectively, for the same parameters. Due to the limited availability of experimenttal and parametric studies in nanofluid applications, Colak et al. [29] evaluated the use of an AI-based approach to estimate key performance parameters. Utilising six input variables, the model achieved deviation rates of -0.66%, 0.001%, and 0.12% for the respective outputs, demonstrating the method's effectiveness in compensating for the lack of empirical data.

Shell and helically coiled tube heat exchangers are increasingly utilised in industrial applications due to their compact design and enhanced heat transfer surface area compared to conventional models. In the study conducted by Çolak et al. [30], two distinct ANN architectures were developed using a dataset of 105 samples. These models were designed to predict key output parameters, including the heat transfer coefficient, pressure drop, Nusselt number, and performance evaluation criteria. In recent study by Çolak et al. [31], an ANN was employed to predict the Nusselt number, friction factor and performance evaluation criteria for heat transfer in straight corrugated tubes, based on flow rate and corrugation parameters. The model was specifically developed to estimate the flow and thermal behaviour of corrugated tubes operating at low flow rates. This proposed approach offers a valuable tool for thermal system applications,

providing accurate predictions that can assist designers in improving system efficiency.

The purpose of this study is to enhance the energy efficiency of climate control systems through the optimisation of earth-toair heat exchanger (EAHE) design and operation using twisted tabs. While EAHEs are well-established for utilising stable subsoil temperatures to moderate indoor climates, their thermal performance can still be significantly improved. However, several critical research challenges persist in the literature. First, the integration of passive flow control devices, such as twisted tabs, into EAHE systems remains underexplored, with limited numerical or experimental investigations of their effect on flow structure and heat transfer. Second, traditional CFD-only approaches, while accurate, are often computationally expensive and impractical for real-time design or operational optimisation. Third, there is a lack of scalable, predictive frameworks that combine physical modelling with data-driven techniques to address performance variability across diverse environmental and geometric conditions.

To address these gaps, this study introduces a dual-strategy approach that combines passive geometric enhancement with advanced data-driven modelling. Specifically, twisted tabs are employed within the EAHE ducts to enhance airflow turbulence and improve thermal exchange between ambient air and surrounding soil. In parallel, a hybrid framework combining (CFD) simulations with (ML) algorithms is developed to predict and optimise thermodynamic performance. This integrated methodology offers a scalable and practical solution for real-time performance assessment and efficient HVAC system design in modern sustainable buildings.

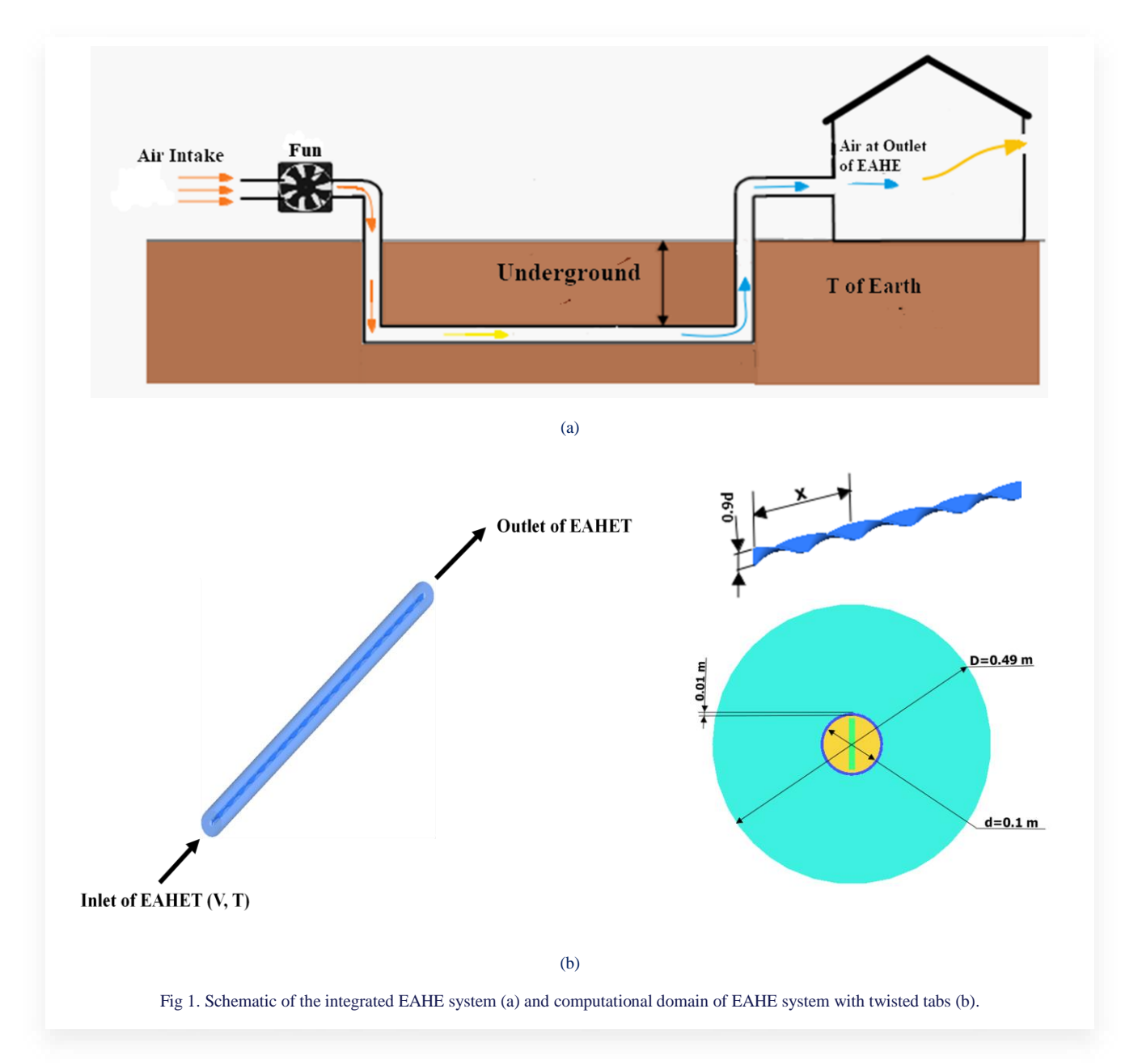
2. Materials and methods

2.1. Geometry and input description

2.1.1. Computational setup

To analyse the complex airflow and heat transfer phenomena within an earth—air heat exchanger (EAHE) system, this study adopts the geometric configuration proposed by Bansal et al. [32] as a baseline reference. A schematic of the investigated EAHE setup is provided in Fig. 1. The system comprises a polyvinyl chloride (PVC) pipe horizontally buried at a depth of 2.7 meters below the ground surface, with an inner diameter of 0.15 meters and a total length of 23.42 meters.

At the inlet, ambient air is introduced into the pipe with a uniform velocity of 5 m/s, a temperature of 42°C, and a turbulence intensity of 5%, consistent with typical hot and arid climatic conditions. The outlet boundary is treated as a pressure outlet with zero gauge pressure, allowing for fully developed flow. The pipe wall is assumed to be thermally conductive, allowing heat exchange between the airflow and the surrounding soil. The outer soil boundary is modelled as a fixed temperature boundary, based on the annual average subsoil temperature at the burial depth. No-slip conditions are applied to all solid surfaces.



The simulation employs the standard k– ε turbulence model, selected for its enhanced performance in capturing swirling and recirculating flows, as commonly observed in EAHE applications. The residual convergence criteria for all transport equations are set to 10^{-6} to ensure numerical stability and accuracy. Furthermore, the working fluid (air) is treated as an incompressible ideal gas, and the surrounding soil is assumed homogeneous with constant thermal properties. This study investigates a novel configuration of an (EAHET), wherein twisted tabs are inserted within the inner tube to enhance thermal performance. As depicted in Fig. 1, the twisted tabs are strategically placed along the inner wall of the tube to promote turbulence and improve heat transfer between the air and the surrounding soil. The analysis explores the impact of the number of twisted tabs, specifically 2, 5, 10, 15 and 20 tabs, on the system's thermal behaviour. Each configuration is labelled accordingly as EAHET-02, EAHET-05, EAHET-10, EAHET-15 and EAHET-20. In addition to tab quantity, the study examines the influence of different inner tube materials, including polyvinyl chloride (PVC), aluminium (AL) and high-density polyethylene (HDPE), as well as the effect of soil thermal conductivity. These parameters are evaluated through detailed CFD simulations to assess their roles in enhancing the heat transfer efficiency of the EAHET system. The details of thermo-physical properties of air, soil and inner tube materials are presented in Table 1. The temperature selected at the pipe's entrance in these suggested designs is based on the location of our nation; on average, it is around 42°C.

2.1.2. Turbulence model validation

To perform this study, multiple simulations were conducted using ANSYS CFX software [33]. In this solver package, the Reynolds-averaged Navier–Stokes (RANS) equations are solved using the finite volume method to discretise the continuity, momentum, and energy equations. A second-order upwind scheme is applied to solve the momentum, energy, and turbulence model equations. For pressure–velocity coupling, the

Table 1. Properties of materials.

Material	Density [kg/m³]	Specific heat capacity [J/(kg K)]	Thermal conductivity [W/(m K)]		
Air	0.0242	1.225	1006		
PVC	1380	900	0.16		
HDPE	940	2000	0.4		
AL	2702	903	237		
Soil 1	2050	1840	0.52		
Soil 2	2215	1260	1.26		
Soil 3	1700	906	2.1		

SIMPLEC algorithm [34] is employed. The governing equations, which represent the conservation of mass, momentum, and energy, are expressed as follows [35]:

$$\frac{\partial(\rho u_i)}{\partial x_i} = 0,\tag{1}$$

$$\rho \bar{u}_j \frac{\partial \bar{u}_i}{\partial x_j} = -\frac{\partial \bar{p}}{\partial x_i} + \frac{\partial}{\partial x_j} \left[\mu \left(\frac{\partial \bar{u}_i}{\partial x_j} + \frac{\partial \bar{u}_j}{\partial x_i} \right) - \overline{\rho u_i' u_j'} \right], \tag{2}$$

$$\frac{\partial}{\partial x_i}(\rho u_i T) = \frac{\partial}{\partial x_i} \left[\left(\frac{\lambda}{c_p} + \frac{\mu_t}{P r_t} \right) \frac{\partial T}{\partial x_i} \right], \tag{3}$$

where p is the pressure, T is the temperature and u_i represents the velocity component in the i-th direction. Parameter c_p represents the specific heat capacity, ρ is the density, λ is the thermal conductivity, μ_t and Pr_t are the turbulent viscosity and turbulent Prandtl number, respectively.

Modelling of the Reynolds stresses $(-\rho \overline{u_i'u_j'})$ in Eq. (2) is done using the Boussinesq hypothesis [36], which relates the Reynolds stresses to the mean velocity gradients via the following equation:

$$-\rho \overline{u_i' u_j'} = \mu_t \left(\frac{\partial u_i}{\partial x_i} + \frac{\partial u_j}{\partial x_i} \right) - \frac{2}{3} \left(\rho k + \mu_t \frac{\partial u_i}{\partial x_i} \right) \delta_{ij}. \tag{4}$$

Turbulent quantities in the Navier–Stokes equations are treated using the turbulent viscosity μ_i , which is given by:

$$\mu_t = \rho C_{\mu} \frac{k^2}{\varepsilon}, \quad C_{\mu} = 0.085.$$

According to the literature, this choice aligns with several recent CFD-based EAHE studies. For instance, Rahimi et al. [14] and Bansal et al. [32] utilised k– ε -based turbulence models and obtained reliable predictions of temperature distribution and energy efficiency. In the present study, the standard k– ε model effectively captured the axial temperature decay and overall heat exchange behaviour, while maintaining reasonable computational costs for long-duration simulations. Additionally, the k– ε model exhibited good agreement with experimental data by accurately representing turbulent flow characteristics and predicting heat transfer rates, making it well-suited for assessing the thermal performance of EAHE systems under complex flow conditions.

The governing transport equations for the turbulent kinetic energy (k) and its dissipation rate (ε) are solved using the RNG

 $k-\varepsilon$ turbulence model, which provides enhanced accuracy for flows with strong streamline curvature and high strain rates, such as in film-cooling jets. The general form of these equations can be expressed as follows:

$$\frac{\partial}{\partial t}(\rho k) + \frac{\partial}{\partial x_{j}}(\rho k u_{j}) = \frac{\partial}{\partial x_{j}} \left[\left(\mu \frac{\mu_{t}}{\sigma_{k}} \right) \frac{\partial k}{\partial x_{j}} \right] + P_{k} + P_{kb} - \rho \varepsilon, (5)$$

$$\frac{\partial}{\partial t}(\rho \varepsilon) + \frac{\partial}{\partial x_{j}}(\rho \varepsilon u_{j}) = \frac{\partial}{\partial x_{j}} \left[\left(\mu \frac{\mu_{t}}{\sigma_{\varepsilon}} \right) \frac{\partial \varepsilon}{\partial x_{j}} \right] + \frac{\varepsilon}{k} (C_{\varepsilon 1} P_{k} - \rho C_{\varepsilon 2} \varepsilon + C_{\varepsilon 1} P_{\varepsilon b}), \quad (6)$$

$$P_k = \mu_t \left(\frac{\partial u_i}{\partial x_j} + \frac{\partial u_j}{\partial x_i} \right) \frac{\partial u_i}{\partial x_j} - \frac{2}{3} \frac{\partial u_k}{\partial x_k} \left(3\mu_t \frac{\partial u_k}{\partial x_k} + \rho k \right), \tag{7}$$

where P_{kb} and $P_{\varepsilon b}$ stand for the buoyancy forces' influence. The turbulence caused by viscous forces, or P_k , is represented by the following model:

$$P_k = \mu_t \left(\frac{\partial u_i}{\partial x_j} + \frac{\partial u_j}{\partial x_i} \right) \frac{\partial u_i}{\partial x_j} - \frac{2}{3} \frac{\partial u_k}{\partial x_k} \left(3\mu_t \frac{\partial u_k}{\partial x_k} + \rho k \right). \tag{8}$$

The empirical constants used in the RNG $k-\epsilon$ model are summarised in Table 2. These constants are derived from the model calibration and govern the production, dissipation and diffusion of turbulence quantities within the computational domain.

Table 2. The RNG k– ε turbulence model constants.

Symbol $C_{\varepsilon 1}$ $C_{\varepsilon 2}$ C_{μ} σ_{k} σ_{ε} Value 1.44 1.92 0.09 1.0 1.3

The heat transfer coefficient (h) is expressed as:

$$h = \frac{Q_C}{\pi dL(T_{in} - T_{out})},\tag{9}$$

where Q_C is the total thermal energy extracted from the air, d and L is the inner diameter and length of EAHE, respectively; the fluid temperatures at the inlet and outlet are T_{in} and T_{out} , respectively.

2.1.3. Grid independence study

The transient temperature field surrounding the horizontally buried pipe of the EAHE system was analysed using an unstructured grid and CFD-based modelling. As seen in Fig. 2, temperature gradients are more noticeable close to the pipe wall, thus a denser mesh was used there and a coarser one further away. To predict the system's thermal performance and evaluate the cooling capacity of the earth-air heat exchanger, a transient and implicit numerical model was used. This model is based on the coupled simulation of heat transfer and turbulent airflow.

To accurately replicate real conditions and ensure high precision, element type and mesh density were varied according to the temperature sensitivity of each region. As illustrated in Fig. 2a, the number of mesh elements significantly affects the outcome of the CFD analysis. Increasing the element count improves solution quality up to a certain threshold. A mesh with

1.4 million elements was selected for the 54 simulation cases examined in this study. Figure 2b presents the simulated temperature distribution along the length of the PVC pipe. With the exception of the inlet region, the CFD predictions exhibit consistently lower temperature values compared to the corresponding experimental measurements throughout the pipe.

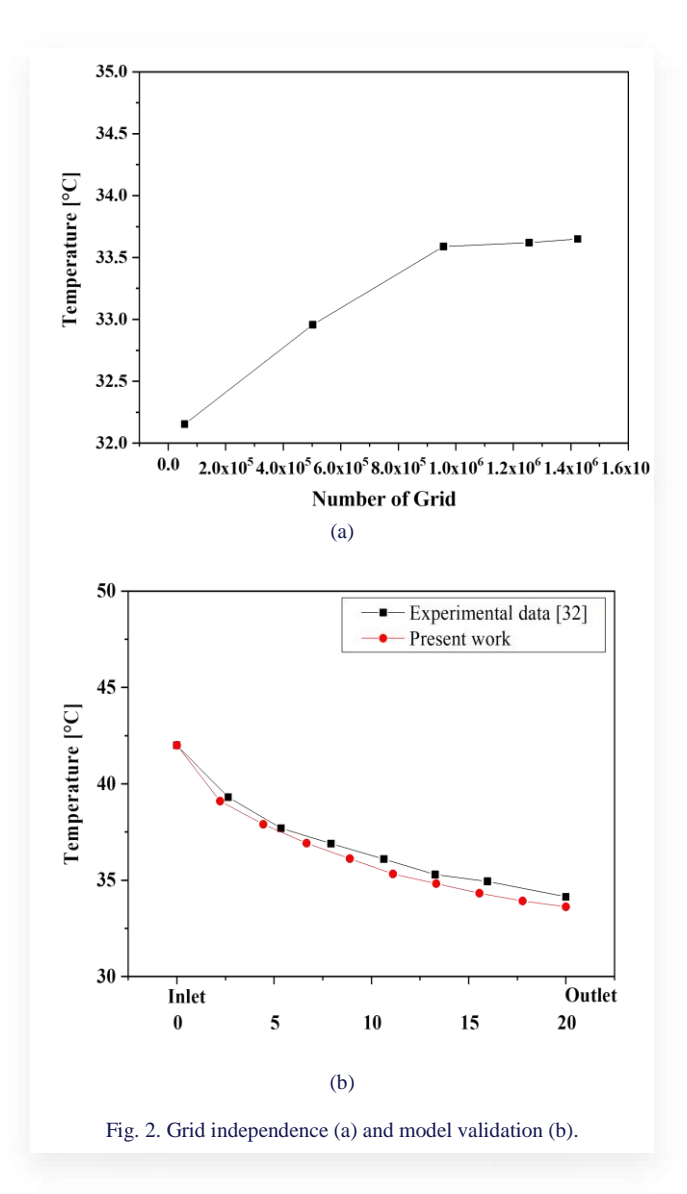
3. Artificial neural network modelling and validation

The goal of this stage is to collect sufficient data to build a comprehensive dataset for training and testing artificial intelligence models. The selected input parameters include the number of twisted tabs, the thermal conductivity (λ) of the soil, and the material of the tube. The outlet air temperature is designated as the output variable. Current machine learning models rely on small datasets for training, enabling more effective extraction of patterns and relationships within the data. This approach enhances the model's generalization ability, simplifies data collection and reduces the time required for numerical simulations.

3.1. Methodology

Boundary conditions obtained from numerical simulations are commonly used as input parameters for machine learning prediction models (Vu et al. [37], Chen et al. [38]). Traditional models typically require large datasets generated through extensive simulations to effectively capture the underlying patterns and relationships in the system. In contrast, the current study demonstrates that high predictive performance can be achieved using only 216 data points. Despite the limited dataset, the machine learning models showed excellent accuracy when tested against the observed data.

The goal of this stage is to collect sufficient data to build a comprehensive dataset for training and testing artificial intelligence models. The selected input parameters include the number of twisted tabs, the thermal conductivity (λ) of the soil and the material of the tube, while the outlet air temperature is des-



ignated as the output variable. As illustrated in Fig. 3, the machine learning workflow involves data pre-processing, model training using algorithms, such as decision tree (DT), SVR and

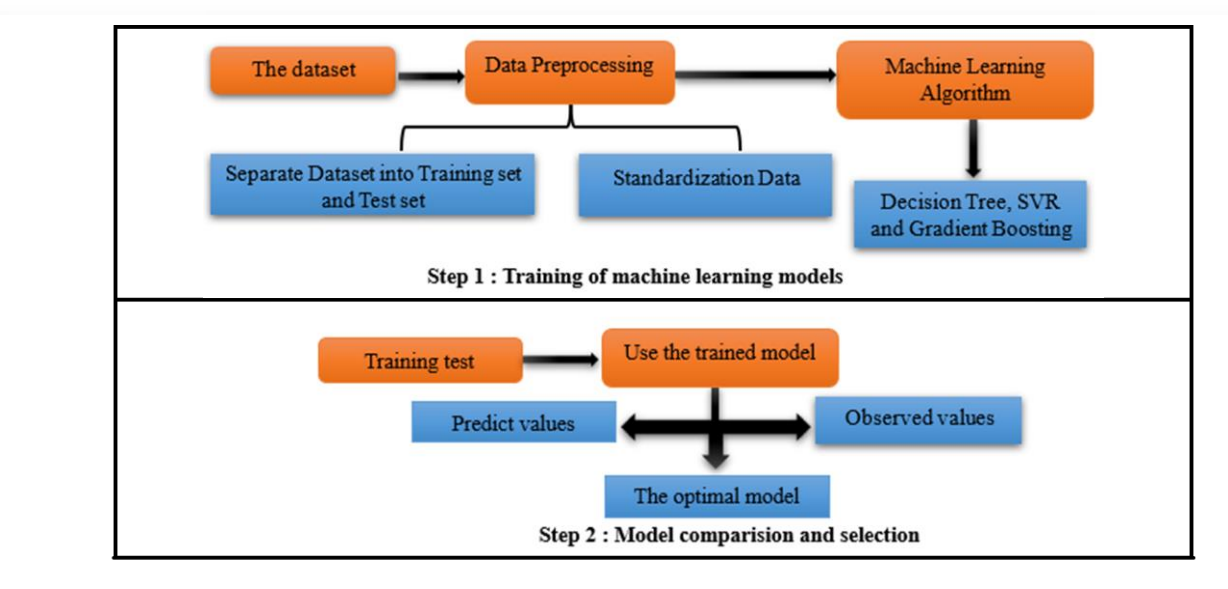


Fig. 3. Flowchart explaining the methodology.

gradient boosting (GB), and subsequent model evaluation and selection. Current machine learning models rely on small datasets for training, enabling more effective extraction of patterns and relationships within the data. This approach enhances the model's generalisation ability, simplifies data collection, and reduces the time required for numerical simulations.

3.2. Data preparation for training

Before training a machine learning model, it is essential to preprocess the dataset to ensure optimal performance. In this study, standardisation was applied, which is a common feature scaling method. Standardisation transforms the data so that it has a mean of 0 and a standard deviation of 1, ensuring that all features contribute equally to the model, regardless of their original scales [39,40]. The data were transformed using the following standardisation equation:

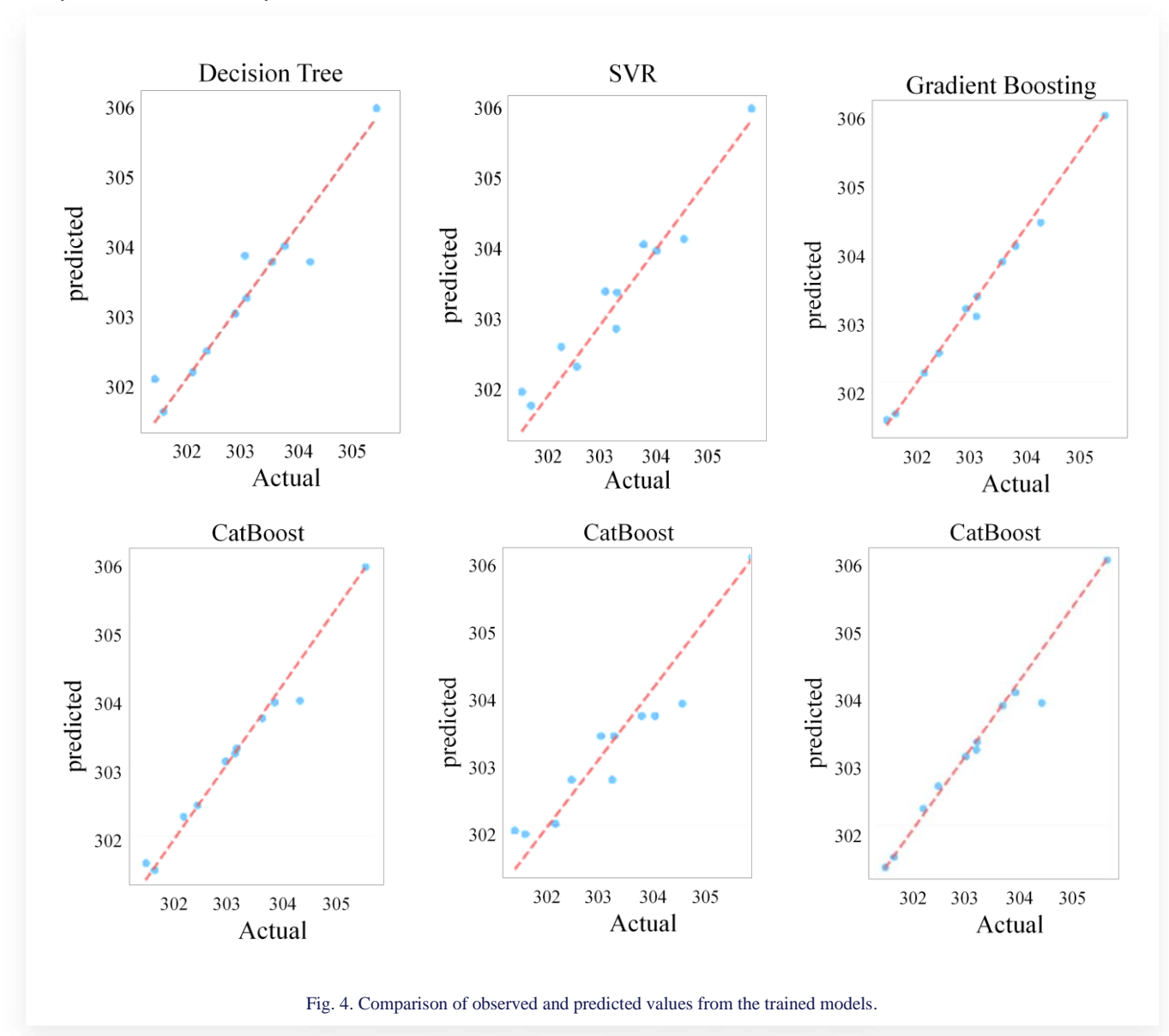
Standardised value =
$$\frac{\text{original value-mean value}}{\text{standard deviation}}$$
. (10)

For this research, multiple predictive models were evaluated, and only three models, namely DT, SVR and GB, were chosen

based on their accuracy. The model that is selected for this study is the gradient boosting model. Prior studies have suggested that gradient boosting is effective in working with smaller datasets (Jiang et al. [41], Lubke et al. [42], Cha et al. [43]).

Gradient boosting is a unique example of ensemble learning in machine learning that is well known for its accuracy in performing regression tasks is gradient boosting. It uses the predictions of several weak learners, typically decision trees, to create a strong predictive model. The strategy is to build models iteratively, where every new model attempts to minimise the error left by its previous counterpart by fitting it to the residuals (errors) of a pre-existing ensemble, thereby minimising a chosen metric, for instance, mean squared error. Gradient boosting is popular because of its effectiveness with many types of data and also because it reveals the most important features to be considered, making the task of finding key factors in the data quite easy and straightforward.

Figure 4 presents a comparison between actual and predicted values across six machine learning models. Ensemble methods such as GB, CatBoost, and XGBoost exhibit strong agreement



MODEL	RM	ISE	MAE		NSE / R ²	
	Train Dataset	Test Dataset	Train Dataset	Test Dataset	Train Dataset	Test Dataset
SVR	0.2629	0.3175	0.1790	0.2768	0.9776	0.9333
SVR, Gong et al. [48]	0.3647	0.30	0.2169	0.2331	0.9579	0.9611
Decision tree	0.0126	0.3531	0.102	0.2011	0.9661	0.9175
RF, Gong et al. [48]	0.2868	0.3151	0.178	0.2335	0.9740	0.9572
Gradient boosting	0.0188	0.01032	0.0138	0.0612	0.9999	0.9930
LGBM, Gong et al. [48]	0.1929	0.2856	0.134	0.2242	0.9882	0.9648

with the ideal prediction line, validating their credibility in capturing the data trends accurately. In contrast, although SVR and DT exhibit some deviation from the reference line, they still demonstrate satisfactory performance in this study, proving to be effective modelling tools. Despite their limitations, they contribute valuable insights and remain relevant within the scope of the analysis.

The training set comprises 80% of the total data, while the remaining 20% is allocated for testing the model's performance. This split is done prior to any pre-processing, such as standardisation, to prevent data leakage and ensure that the model's evaluation is unbiased and reflects its true generalisation capability [44]. The model's performance is checked using a line graph of the data fit and three key evaluation measures. These measures are root mean squared error (RMSE) [45], mean absolute error (MAE) [46], and the Nash-Sutcliffe efficiency (NSE) [47]. These methods are well-known and often used to assess how well machine learning models make predictions. This quantitative comparison shows that the GB model developed in this work not only outperforms other models used in this study (e.g. SVR, DT), but also clearly exceeds the performance of existing traditional or physics-based models reported in the literature. This affirms the robustness and accuracy of the GB model for modelling the thermal behaviour of earth-air heat exchangers (EAHEs), especially when enhanced with integrated twisted tabs.

In terms of goodness of fit, the GB model achieved an NSE/R² value of 0.9930 on the test set, which is higher than the 0.9648 reported for light gradient boosting machine (LGBM) in and 0.9572 for random forest (RF) in [48], and 0.9611 for SVR, highlighting its superior ability to capture the variance in the data.

The results presented in Table 3 clearly demonstrate the superior predictive performance of the GB model compared to both the other machine learning models evaluated in this study and the traditional/physics-based models reported in the literature [48]. During the testing phase, the GB model achieved the lowest RMSE of 0.1032 and MAE of 0.0612, outperforming Gong et al.'s LGBM model, which yielded an RMSE of 0.2856 and an MAE of 0.2242. Similarly, in the training phase, the GB model achieved an RMSE of 0.0188 and an MAE of 0.0138, which are significantly better than those reported for the LGBM (0.1929 and 0.134, respectively), and much lower than the SVR (0.3647, 0.2169) and RF (0.2868, 0.178) models in [48].

4. Results and discussion

Twisted tabs are incorporated into (EAHEs) to improve their thermal performance. As depicted in Fig. 5, these internal elements alter the heat transfer characteristics by increasing the effective surface area for thermal exchange and enhancing convective flow. The inclusion of twisted tabs leads to a noticeable improvement in the heat transfer coefficient when compared to the baseline configuration without inserts. However, this enhancement does not scale linearly with the number of tabs. Beyond a certain threshold, the increasing number of twisted tabs induces excessive turbulence within the airflow, which, while initially beneficial, ultimately results in reduced residence time of the air in contact with the heat transfer surface. Consequently, the thermal exchange efficiency begins to deteriorate despite higher turbulence levels. Furthermore, the system may reach a state of excessive mixing, wherein the intensification of turbulence ceases to contribute positively to thermal performance and may even become counterproductive.

The graphs in Fig. 6 illustrate the temperature variation along the normalised length of the tube for various tube materials (PVC, HDPE and AL) and six different design

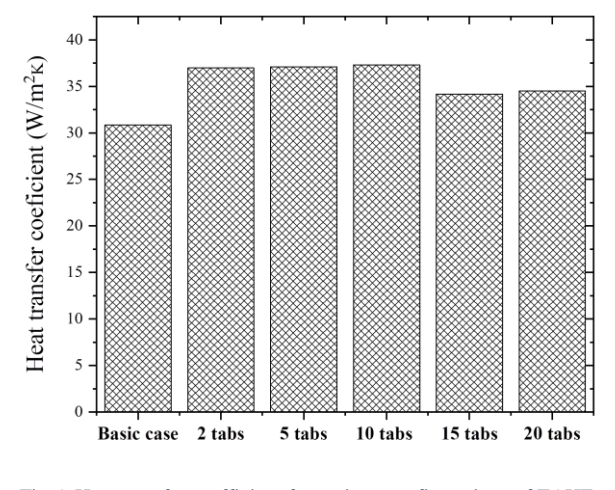
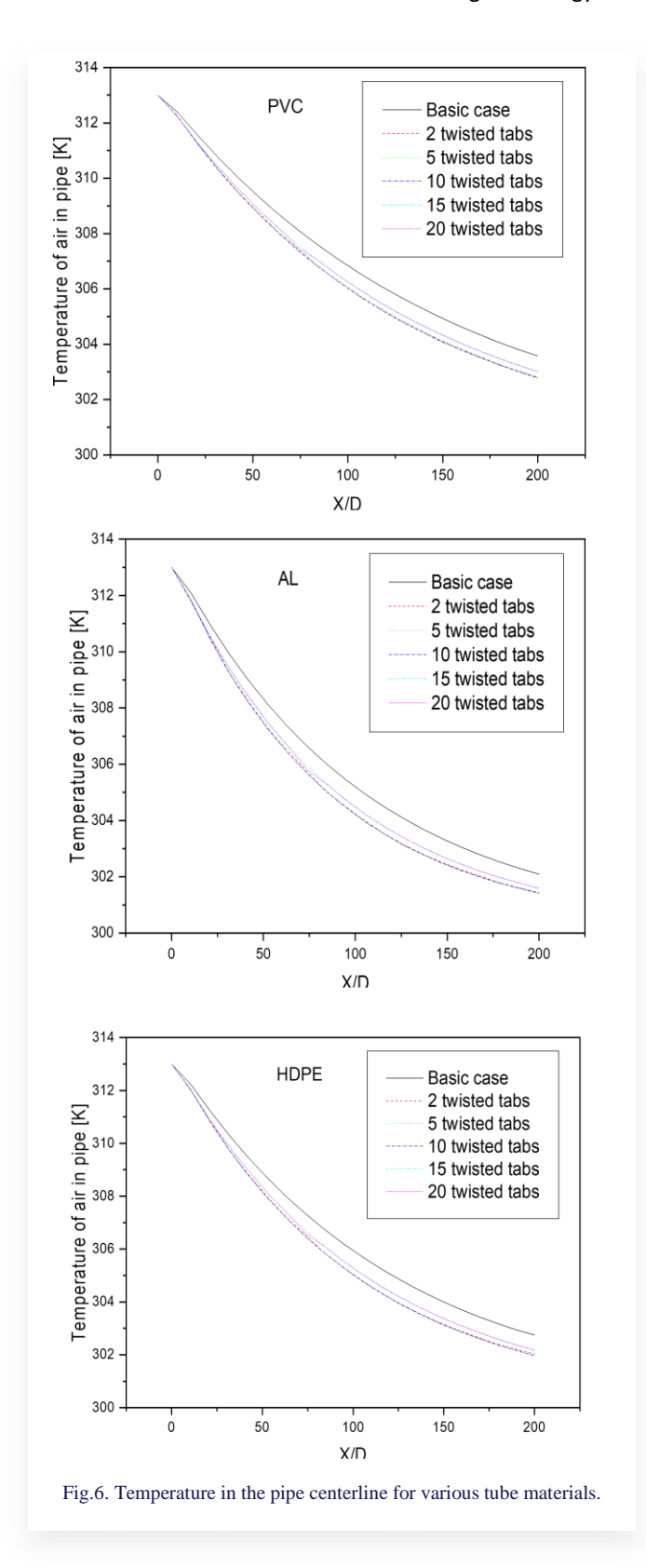


Fig.5. Heat transfer coefficient for various configurations of EAHE.

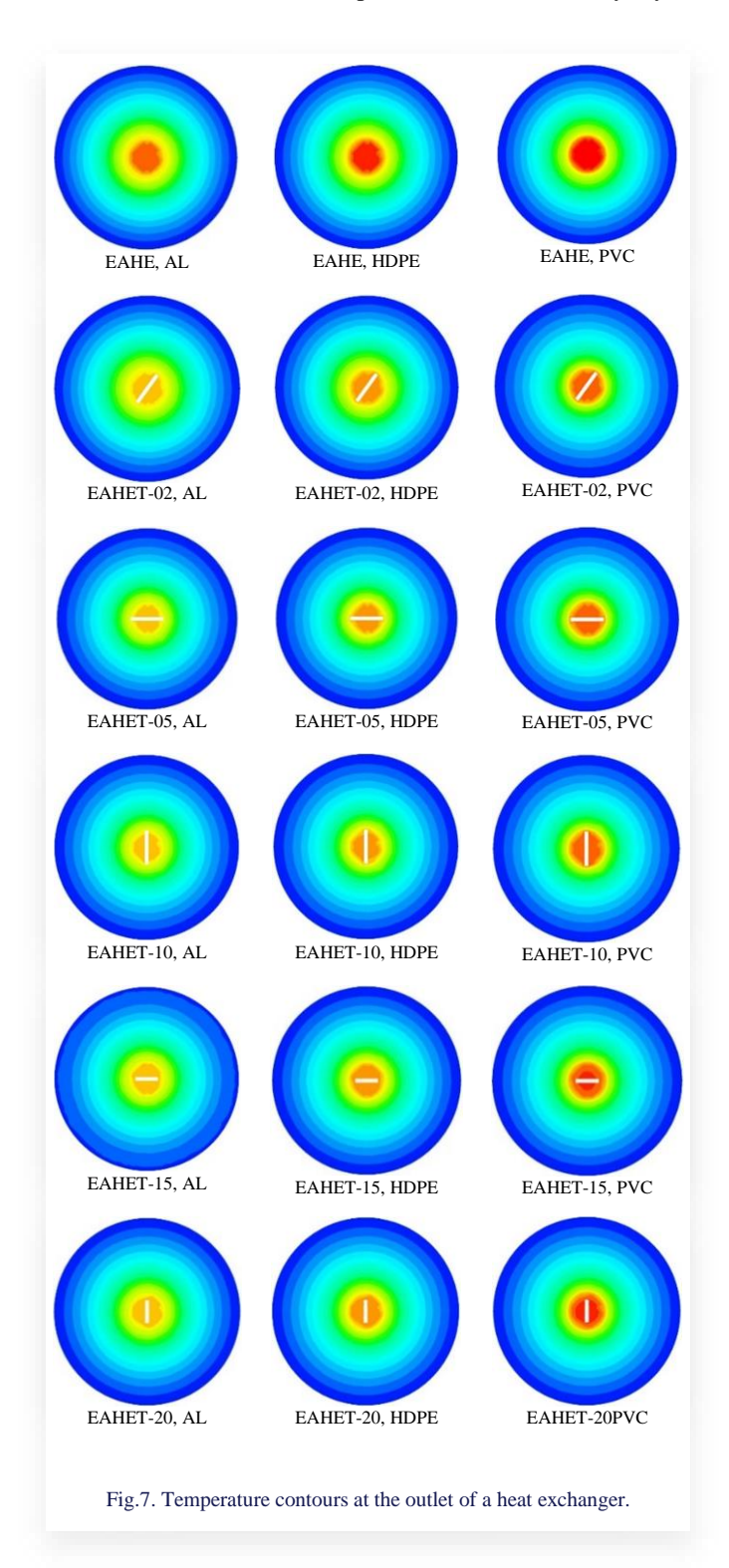
configurations, all evaluated under the same soil condition (soil 3). The temperature profiles consistently show a decline with increasing x/L, indicating progressive cooling of the airflow along the tube. Notably, all five modified configurations



yield lower outlet temperatures compared to the basic case, which can be attributed to the enhanced turbulence and improved convective heat transfer resulting from the incorporation of twisted tabs. As only soil 3, characterised by a relatively high thermal conductivity (see Table 1), was considered in this analysis, its pronounced effect on the thermal performance of the EAHE system is evident. Higher conduc-

tivity facilitates more efficient heat exchange between the subsurface soil and the air flowing through the tube, thereby improving the overall cooling effectiveness of the system.

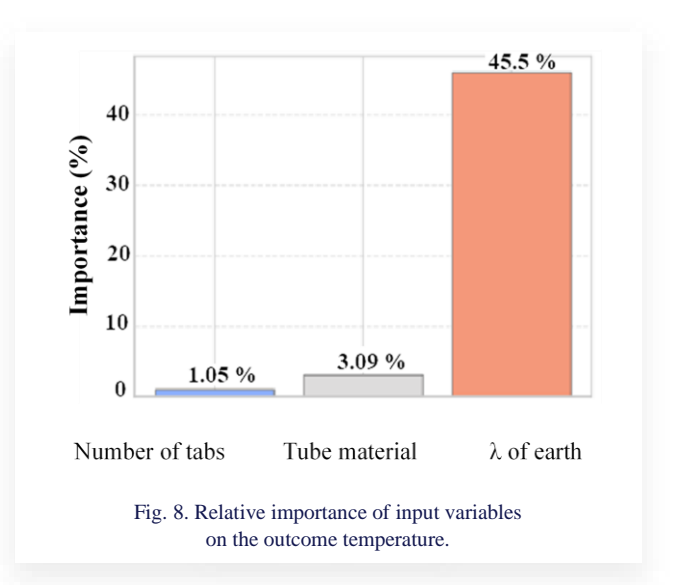
Figure 7 illustrates the temperature contours at the outlet of a heat exchanger, emphasising the impact of incorporating a twisted tab within the inner tube. The presence of twisted tabs generates vortices along their surfaces, which enhances turbulence in the airflow, disrupts the thermal boundary layer,



and promotes better mixing between hotter and cooler regions. As depicted in the figure, the flow contours in the basic case without twisted tabs are more irregular and display cooler regions at the outlet. This indicates less effective heat transfer, primarily due to the presence of laminar flow near the tube walls. This behaviour is consistently observed across the three tube materials studied: PVC, HDPE and AL.

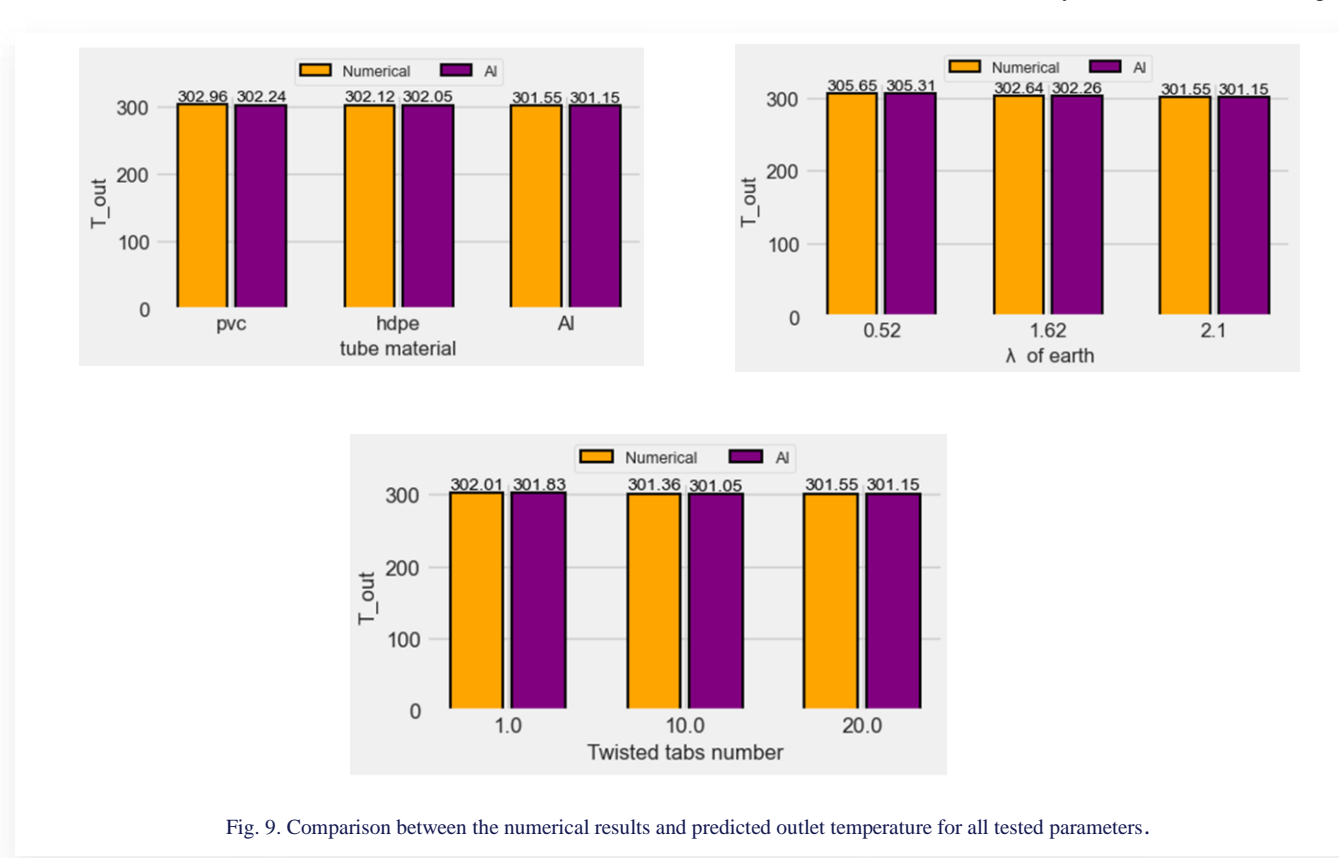
The effectiveness of incorporating twisted tabs into the EAHE system (referred to as EAHETs) is evident in the temperature contours, where the temperature difference between the inlet and outlet can reach up to 7°C. This cooling effect can be further enhanced with extended system operation. Additionally, Fig. 7 highlights the influence of tube materials on the performance of both EAHE and EAHET systems. Among the tested materials, the aluminium tube yielded the lowest outlet temperature. This indicates that the combination of high thermal conductivity and the presence of twisted tabs significantly improves heat transfer. The twisting of the wall promotes enhanced fluid mixing, maintaining a strong temperature gradient near the tube surface and thereby increasing the overall heat exchange efficiency.

Figure 8 illustrates the findings of the sensitivity analysis, which quantifies the relative impact of various input parameters on the outlet air temperature of the (EAHE) system. Among the examined factors, the thermal conductivity (λ) of the surrounding soil emerges as the most influential, contributing approximately 45.5% to the variation in outlet temperature. This substantial influence underscores the critical role of soil thermal properties in governing heat exchange between the buried pipe and its environment. In contrast, the effects of the pipe material and the number of internal twisted tabs are markedly less signif-



icant, accounting for only 3.09% and 1.05%, respectively. The comparable and minimal contributions of these two variables highlight their secondary roles relative to soil conductivity. These findings suggest that while geometric and material modifications within the EAHE system can offer marginal performance improvements, optimising the thermal characteristics of the soil environment should be prioritised for maximising system efficiency.

Figure 9 presents a comparative analysis between the actual outlet temperatures (T_{out}) obtained through numerical simulations of the EAHE system and those predicted by the GB machine learning model. Each subfigure corresponds to distinct combinations of system parameters, including the type of pipe material, the thermal conductivity (λ) of the surrounding soil,



and the number of twisted tab inserts within the pipe. The predicted temperature values exhibit a strong correlation with the simulated results across all parameter configurations. This high level of agreement underscores the GB model's robustness, accuracy, and reliability in capturing complex nonlinear interactions within the system, thereby validating its potential as a powerful predictive tool for evaluating EAHE performance.

4.1. Industrial applicability and scalability

The present study proposes a hybrid approach combining computational fluid dynamics (CFD) and machine learning (ML) to evaluate and optimise twisted tab-based earth-air heat exchangers (EAHEs).

The configuration is particularly important in industrial and commercial buildings needing sustainable and passive cooling strategies. The design results have direct implications for actual HVAC and green building systems, where sub-surface temperature can be used to pre-condition ventilation air. The twisted tabs added improve air-side turbulence and augment heat exchange with the adjacent soil, rendering the system viable in high-density city centres with limited areas of land for installation of conventional cooling devices. At a scalability level, the datasets generated by CFD that are employed to train the ML models can be scaled across a broader span of operating conditions, geometries and soil properties. The trained models, especially ensemble learners XGBoost and CatBoost, produced excellent prediction precision with minimal computational overhead and can therefore be employed for integration into industrial control systems, real-time monitoring platforms or digital twins. Furthermore, these ML models are platform-agnostic and lightweight, making them deployable on embedded systems or cloud platforms for large-scale monitoring and optimisation. Subsequent research can examine integrating these models with SCADA systems or building energy management systems (BEMS) to support automated, real-time decision-making for energy-efficient operation.

5. Conclusions

This study presented a numerical and data-driven hybrid approach to examine and optimise the thermal performance of an earth-air heat exchanger (EAHE) system equipped with twisted tab inserts. A dataset of 216 entries from CFD simulations was used to train and test various machine learning (ML) models. The originality of this study lies in the integration of turbulence-inducing geometrical modifications with predictive ML models for the enablement of rapid performance analysis of EAHE configurations.

The key findings are summarised as follows:

 CFD analysis, including temperature contour plots and profiles, centreline revealed that twisted tabs significantly enhance convective heat transfer. This is attributed to the generation of localised turbulence and thermal boundary layer disruption, thereby leading to better thremal mixing and increased energy exchange. These enhancements are beneficial to the performance of the EAHE in both heating and cooling modes;

- Among the ML algorithms tried (DT, SVR and GB), GB
 worked better than the others in predictive accuracy. It
 learned nonlinear interactions between input parameters
 nicely and offered a good surrogate model for the rapid
 and accurate prediction of EAHE performance parameters.
- Sensitivity analysis revealed soil thermal conductivity (λ) as the most influential parameter on system efficiency. Though the tube material and the number of twisted tabs both played a secondary individual effect (4.14%), they remain important design parameters for optimising system performance by internal geometry and material selection.

Overall, this study demonstrates that the combination of CFD simulations and machine learning provides an effective framework for EAHE system analysis and optimisation. While the results are promising, limitations include the use of steady-state simulations and a static geometric range. Transient flow regimes, longer datasets with a wider variety of geometries, and experimental validation should be the focus of future work to enhance model generalizability even further. In addition, the deployment of trained ML models within real-time building control systems can open doors towards adaptive and energy-saving climate control.

References

- [1] Alrwashdeh, S.S., Ammari, H., Madanat, M.A., & Al-Falahat, A.M. (2022). The Effect of Heat Exchanger Design on Heat Transfer Rate and Temperature Distribution. *Emerging Science Journal*, 6(1), 128–137. doi: 10.28991/esj-2022-06-01-010
- [2] Bejan, A., Alalaimi, M., Lorente, S., Sabau, A., & Klett, J. (2016). Counterflow heat exchanger with core and plenums at both ends. *International Journal of Heat And Mass Transfer*, 99, 622–629. doi: 10.1016/j.ijheatmasstransfer.2016.03.117
- [3] Kareem, Z.S., Jaafar, M.M., Lazim, T.M., Abdullah, S., & Abdulwahid, A.F. (2015). Passive heat transfer enhancement review in corrugation. *Experimental Thermal and Fluid Science*, 68, 22–38. doi.org/10.1016/j.expthermflusci.2015.04.012
- [4] Liu, S., & Sakr, M. (2013). A comprehensive review on passive heat transfer enhancements in pipe exchangers. *Renewable and Sustainable Energy Reviews*, 19, 64–81. doi: 10.1016/j.rser.2012. 11.021
- [5] Aziz, A., & Rehman, S. (2020). Analysis of non-equidistant baffle spacing in a small shell and tube heat exchanger. *Archives of Thermodynamics*, 41(2), 201–221. doi: 10.24425/ather.2020. 133629
- [6] Muszyński, T., & Dorao, A. (2019). Heat transfer and pressure drop characteristics of the silicone-based plate heat exchanger. Archives of Thermodynamics, 40(1), 127–143. doi: 10.24425/ ather.2019.128294
- [7] Serrao, P., Pawase, H., Prakash, A., & Pandita, V. (2017). Comparison of overall heat transfer coefficient in plain and corrugated pipe and it's CFD analysis. *International Journal of Advances in Engineering & Technology*, 10(4), 523–540.
- [8] Vignesh, S., Moorthy, V.S., & Nallakumarasamy, G. (2017). Experimental and CFD analysis of concentric dimple tube heat exchanger. *International Journal of Emerging Technologies in Engineering Research (IJETER)*, 5(7), 18–26.

- [9] Wang, Z., Wang, Y., Zhang, J., Li, S., & Xu, Y. (2022). Numerical Simulation of Heat Transfer Performance of a Dimpled Tubular Heat Exchanger. *Applied Sciences*, 12(24), 12965. doi: 10.3390/app122412965
- [10] Kumar, P.M., & Chandrasekar, M. (2019). CFD analysis on heat and flow characteristics of double helically coiled tube heat exchanger handling MWCNT/water nanofluids. *Heliyon*, 5(7), e02030. doi.org/10.1016/j.heliyon.2019.e02030
- [11] Khan, A., Shah, I., Gul, W., Khan, T.A., Ali, Y., & Masood, S.A. (2023). Numerical and Experimental Analysis of Shell and Tube Heat Exchanger with Round and Hexagonal Tubes. *Energies*, 16(2), 880. doi: 10.3390/en16020880
- [12] Kishan, R., Singh, D. & Sharma, A.K. (2020). CFD Analysis of Heat Exchanger Models Design Using Ansys Fluent. *Internatio-nal Journal of Mechanical Engineering and Technology*, 11(2), 1–9. doi: 10.34218/IJMET.11.2.2020.001
- [13] Sharma, S., Sharma, S., Singh, M., Singh, P., Singh, R., Maharana, S., Khalilpoor, N., & Issakhov, A. (2021). Computational Fluid Dynamics Analysis of Flow Patterns, Pressure Drop, and Heat Transfer Coefficient in Staggered and Inline Shell-Tube Heat Exchangers. *Mathematical Problems in Engineering*, 2021, 6645128. doi: 10.1155/2021/6645128
- [14] Rahimi, M., Shabanian, S.R., & Alsairafi, A.A. (2009). Experimental and CFD studies on heat transfer and friction factor characteristics of a tube equipped with modified twisted tape inserts. *Chemical Engineering And Processing Process Intensification*, 48(3),762–770. doi: 10.1016/j.cep.2008.09.07
- [15] Larwa, B., & Kupiec, K. (2020). Principles of modelling of slinky-coil ground heat exchangers. *Chemical And Process Engi*neering New Frontiers, 41(2). doi: 10.24425/cpe.2019.130225
- [16] Molcrette, V., & Autier, V. (2020). New expression to calculate quantity of recovered heat in the earth-pipe-air heat-exchanger operating in winter heating mode. *Archives of Thermodynamics*, 41(2), 103–117. doi: 10.24425/ather.2020.133624
- [17] Ahmad, S.N., & Prakash, O. (2022). Thermal performance evaluation of an earth-to-air heat exchanger for the heating mode applications using an experimental test rig. *Archives of Thermodynamics*, 43(1), 185–207. doi: 10.24425/ather.2022.140931
- [18] Suenaga, D., Takase, Y., Abe, T., Orita, G., & Ando, S. (2023). Prediction accuracy of Random Forest, XGBoost, LightGBM, and artificial neural network for shear resistance of post-installed anchors. *Structures*, 50, 1252–1263. doi: 10.1016/j.istruc.203.02. 066
- [19] Huang, J., Jin, T., Liang, M., & Chen, H. (2021). Prediction of heat exchanger performance in cryogenic oscillating flow conditions by support vector machine. *Applied Thermal Engineering*, 182, 116053. doi: 10.1016/j.applthermaleng.2020.116053
- [20] Celik, N., Tasar, B., Kapan, S., & Tanyildizi, V. (2023). Performance optimization of a heat exchanger with coiled-wire turbulator insert by using various machine learning methods. *International Journal of Thermal Sciences*, 192, 108439. doi: 10.1016/j.ijthermalsci.2023.108439
- [21] Karami, A., Rezaei, E., Rahimi, M., & Zanjani, M. (2012). Artificial Neural Modeling of the Heat Transfer in an Air Cooled Heat Exchanger Equipped with Butterfly Inserts. *International Energy. Journal*, 13, 21–28.
- [22] Li, Z., Shao, L., & Zhang, C. (2016). Modeling of Finned-Tube Evaporator Using Neural Network and Response Surface Methodology. *Journal of Heat Transfer*, 138(5), 051502. doi: 10.1115/ 1.4032358
- [23] Shojaeefard, M.H., Zare, J., Tabatabaei, A., & Mohammadbeigi, H. (2017). Evaluating different types of artificial neural network structures for performance prediction of compact heat exchanger. *Neural Computing And Applications*, 28(12), 3953-3965. doi: 10.1007/s00521-016-2302-z

- [24] Deb, D., Rajan, H., Kundu, R., & Mohan, R. (2021). CFD and Machine Learning based Simulation of Flow and Heat Transfer Characteristics of Micro Lattice Structures. *IOP Conference Series Earth And Environmental Science*, 850(1), 012034. doi: 10.1088/1755-1315/850/1/012034
- [25] Liao, T., Zhao, C., Wang, H., & Ju, S. (2024). Data-driven design of multilayer hyperbolic metamaterials for near-field thermal radiative modulator with high modulation contrast. *International Journal of Heat And Mass Transfer*, 219, 124831. doi: 10.1016/j.ijheatmasstransfer.2023.124831
- [26] Ren, F., Zhang, F., Zhu, Y., Wang, Z., & Zhao, F. (2024). Enhancing heat transfer from a circular cylinder undergoing vortex induced vibration based on reinforcement learning. *Applied Thermal Engineering*, 236, 121919. doi: 10.1016/j.applthermaleng. 2023.121919
- [27] Wang, C., & Vafai, K. (2024). Heat transfer enhancement for 3D chip thermal simulation and prediction. *Applied Thermal Engineering*, 236, 121499. doi: 10.1016/j.applthermaleng.2023.121499
- [28] Çolak, A.B., Açıkgöz, Ö., Mercan, H., Dalkılıç, A.S., & Wongwises, S. (2022). Prediction of heat transfer coefficient, pressure drop, and overall cost of double-pipe heat exchangers using the artificial neural network. *Case Studies in Thermal Engineering*, 39, 102391. doi: 10.1016/j.csite.2022.102391
- [29] Çolak, A.B., Mercan, H., Açıkgöz, Ö., Dalkılıç, A.S., & Wongwises, S. (2023). Prediction of nanofluid flows' optimum velocity in finned tube-in-tube heat exchangers using artificial neural network. *Kerntechnik*, 88(1), 100–113. doi: 10.1515/kern-2022-0097
- [30] Colak, A.B., Akgul, D., Mercan, H., Dalkılıç, A.S., & Wongwises, S. (2023). Estimation of heat transfer parameters of shell and helically coiled tube heat exchangers by machine learning. *Case Studies in Thermal Engineering*, 42, 102713. doi: 10.1016/j.csite. 2023.102713.
- [31] Çolak, A.B., Kirkar, S.M., Gönül, A., & Dalkilic, A.S. (2024). Assessment of heat transfer characteristics of a corrugated heat exchanger based on various corrugation parameters using artificial neural network approach. *International Journal of Heat and Fluid Flow*, 108, 109455. doi: 10.1016/j.ijheatfluidflow.2024. 109455
- [32] Bansal, V., Misra, R., Agrawal, G.D., & Mathur, J. (2010). Performance analysis of earth–pipe–air heat exchanger for summer cooling. *Energy and Buildings*, 42(5), 645–648. doi: 10.1016/j.enbuild.2009.11.001.
- [33] ANSYS Inc., ANSYS CFX User's Guide, Release 2020 R2, AN-SYS Inc., Canonsburg, Pennsylvania, USA.
- [34] Patankar, S. (2018). Numerical Heat Transfer and Fluid Flow (1st ed.). CRC Press, Boca Raton.
- [35] Versteeg, H.K., & Malalasekera, W. (2007). An Introduction to Computational Fluid Dynamics: The Finite Volume Method (2nd ed.). Pearson Education Limited.
- [36] Wilcox, D.C. (1998). Turbulence Modeling for CFD (3rd ed.). DCW Industries Inc., La Canada, CA.
- [37] Vu, A.T., Gulati, S., Vogel, P., Grunwald, T., & Bergs, T. (2021). Machine learning-based predictive modeling of contact heat transfer. *International Journal of Heat and Mass Transfer*, 174, 121300. doi: 10.1016/j.ijheatmasstransfer.2021.121300
- [38] Chen, X., Zhang, K., Ji, Z., Shen, X., Liu, P., Zhang, L., Wang, J., & Yao, J. (2023). Progress and Challenges of Integrated Machine Learning and Traditional Numerical Algorithms: Taking Reservoir Numerical Simulation as an Example. *Mathematics*, 11(21), 4418. doi: 10.3390/math11214418.
- [39] Maharana, K., Mondal, S., & Nemade, B. (2022). A review: Data pre-processing and data augmentation techniques. *Global Tran*-

- sitions Proceedings, 3(1), 91–99. doi: 10.1016/j.gltp.2022.04.
- [40] Pandey, Y.N., Rastogi, A., Kainkaryam, S., Bhattacharya, S., & Saputelli, L. (2020). Machine Learning in the Oil and Gas Industry (1st ed.). Apress Berkeley, CA.
- [41] Jiang, J., Wang, R., Wang, M., Gao, K., Nguyen, D.D., & Wei, G. (2020). Boosting Tree-Assisted Multitask Deep Learning for Small Scientific Datasets. *Journal of Chemical Information and Modeling*, 60(3), 1235–1244. doi: 10.1021/acs.jcim.9b01184
- [42] Lubke, G., Laurin, C., Walters, R., Eriksson, N., Hysi, P., Spector, T., Montgomery, G., Martin, N., Medland, S., & Boomsma, D. (2013). Gradient Boosting as a SNP Filter: an Evaluation Using Simulated and Hair Morphology Data. *Journal of Data Mining in Genomics & Proteomics*, 4(4), 1000143. doi: 10.4172/2153-0602.1000143
- [43] Cha, G., Moon, H., & Kim, Y. (2021). Comparison of Random Forest and Gradient Boosting Machine Models for Predicting Demolition Waste Based on Small Datasets and Categorical Variables. *International Journal of Environmental Research and Pu*blic Health, 18(16), 8530. doi: 10.3390/ijerph18168530
- [44] Bouke, M.A., Abdullah, A., ALshatebi, S.H., Abdullah, M.T., & Atigh, H.E. (2023). An intelligent DDoS attack detection tree-

- based model using Gini index feature selection method. *Microprocessors and Microsystems*, 98, 104823. doi: 10.1016/j.micpro. 2023.104823
- [45] Chai, T., & Draxler, R.R. (2014). Root mean square error (RMSE) or mean absolute error (MAE)? Geoscientific Model Development Discussions, 7(1), 1525–1534. doi: 10.5194/gmdd-7-1525-2014
- [46] Willmott, C., & Matsuura, K. (2005). Advantages of the mean absolute error (MAE) over the root mean square error (RMSE) in assessing average model performance. *Climate Research*, 30(1), 79–82. doi: 10.3354/cr03007
- [47] Nash, J., & Sutcliffe, J. (1970). River flow forecasting through conceptual models part I — A discussion of principles. *Journal* of *Hydrology*, 10(3), 282–290. doi: 10.1016/0022-1694(70) 90255-6
- [48] Gong, M., Bai, Y., Qin, J., Wang, J., Yang, P., & Wang, S. (2020). Gradient boosting machine for predicting return temperature of district heating system: A case study for residential buildings in Tianjin. *Journal of Building Engineering*, 27, 100950. doi: 10.1016/j.jobe.2019.100950